J. Adhesion Sci. Technol. Vol. 8, No. 3, pp. 249–259 (1994)

A model for adhesion-producing interactions of zinc oxide surfaces with alcohols, amines, and alkenes

ROBERT D. BACH,[1] JOSE L. ANDRÉS,[1,†] JULIA E. WINTER,[1]
H. BERNHARD SCHLEGEL,[1] JAMES C. BALL[2] and JOSEPH W. HOLUBKA[2]

[1]*Department of Chemistry, Wayne State University, Detroit, MI 48202, USA*
[2]*Ford Research Laboratory, Ford Motor Company, Dearborn, MI 48121, USA*

Revised version received 15 October 1993

Abstract—The interactions between paint/adhesive polymers and metal surfaces that are critical for adhesion have been studied theoretically. This study used zinc oxide as a model of a galvanized steel surface, and ammonia, water, and ethylene as models for amino, hydroxy, and unsaturated functionalities in paint/adhesive polymers. *Ab initio* molecular orbital calculations were carried out on zinc oxide and zinc oxide dimer. Geometries were optimized at the HF/3-21G level and relative energies were calculated by CASSCF/3-21G and by MP2 with the DZP basis set of Wachters and Hay. Ethylene forms a stable complex with zinc oxide dimer that has a stabilization energy of 24.9 kcal/mol. Insertion of ethylene into zinc oxide dimer to form a stable six-membered ring adduct occurs with a surprisingly low activation energy of 8.8 kcal/mol. The binding energy of ammonia with zinc oxide dimer is 38.5 kcal/mol and the activation energy for insertion of ammonia forming covalent Zn—NH_2 and O—H bonds is calculated to be 9.6 kcal/mol. Aminolysis of zinc oxide dimer with two ammonia molecules has a predicted barrier height of 6.7 kcal/mol. The transition structure for Zn—O bond rupture with one NH_3 and one H_2O molecule is only 1.5 kcal/mol higher in energy than the reactant cluster. The calculations suggest that alkenes, amines, and alcohols could readily form covalent bonds with the ZnO surface, thereby facilitating adhesion of the polymer containing these functional groups to a galvanized surface.

Keywords: Adhesion model; zinc oxide insertion reaction; *ab initio* molecular orbital calculations.

1. INTRODUCTION

The adhesion of polymeric materials to metallic surfaces is a complex phenomenon that can involve a number of physical and chemical processes. These processes range from mechanical interlocking that is strongly dependent on the degree of surface roughness, to more chemical interactions such as van der Waals attractions, hydrogen bonding, acid–base reactions, and covalent bond formation. Adhesion of polymers to metal surfaces has been studied both theoretically and experimentally. The theoretical studies, however, have been quite limited.

†Present address: Department de Quimica, Universitat Autonoma de Barcelona, 08193 Bellaterra, Catalonia, Spain.

Band calculations have been used to study bonding processes [1, 2]. Similar calculations have been used by Hoffmann to explore the interactions of organic molecules at inorganic surfaces [3]. MNDO calculations have been used to examine the interactions of acrylic monomers with aluminum oxide surfaces [4]. The results of these calculations suggested that a Lewis acid–base process occurs selectively with acrylate functional polymers over methacrylate functional polymers. MNDO calculations have also been used to explore the interaction of dicyandiamide with zinc surfaces [5]. In these latter studies, both experimental and theoretical results suggested that the most important adhesion-promoting interaction of dicyandiamide with zinc involved a reduction reaction involving the elemental zinc not the oxide. However, in view of the results with aluminum oxide, it appears that under some conditions a metal oxide can react with unsaturated or other functional groups. A number of investigations have addressed this issue for interactions with zinc oxide [6].

Defects and electronic structures of interfaces in zinc oxide have been studied using cluster molecular orbital calculations for interactions of this oxide with molecular oxygen [7]. Upon adsorption at a free ZnO interfacial site, molecular oxygen was found to form a deep acceptor. The highest occupied levels are antibonding with respect to the O—O bond in the adsorbed oxygen molecule and therefore are expected to facilitate dissociative oxygen chemisorption. The adsorption of carbon monoxide on zinc oxide surfaces has been using studied molecular orbital calculations in a number of studies [8–10].

In this study, we report on the interaction of zinc oxide and zinc oxide dimer with functional groups typically found in polymeric systems comprising coatings and adhesives. This study was carried out primarily to ascertain the structure and stability of the interfacial intermediates formed in the bonding process.

2. METHOD OF CALCULATION

Molecular orbital calculations were carried out using the Gaussian 92 program system [11a] utilizing gradient geometry optimization [11b]. The geometries of the reactants and transition structures were first determined at the Hartree–Fock (HF) level of theory with 3-21G basis set. Relative energies and barrier heights for the zinc oxide monomer/ethylene system were computed by the CISD method with the 3-21G basis set. In order to ascertain the effect of electron correlation on the energies, second-order Møller–Plesset perturbation theory using the WH basis set described below (MP2/WH; frozen core) was used to calculate energies for the zinc oxide dimer systems. All stationary points were characterized as either minima (zero imaginary frequencies) or first-order transition states that exhibited a single imaginary frequency at the HF/3-21G level.

The zinc atom basis sets are the 3-21G basis set reported by Dobbs and Hehre [12]. The Wachters–Hay DZP basis set consists of the [8*s*, 6*p*, 2*d*] contraction of the (14*s*, 11*p*, 5*d*) primitive set of Wachters [13a] augmented by two diffuse *p* functions (exponents = 0.16, 0.05) and a 3*d* diffuse function [13b, c] (exponent = 0.15). The basis set in this form has 46 basis functions per zinc atom and is referred to as the WH basis set. The O, N, and H basis sets are the double zeta Huzinaga–Dunning [13d, e] supplemented with *d* functions on N and O.

3. RESULTS AND DISCUSSION

3.1. Electronic structure of zinc oxide

We initiated this study with the monomer of zinc oxide at the RHF/3-21G level. The closed shell description of ZnO predicts a Zn—O bond distance of 1.679 Å. The wave function shows an RHF→UHF instability (root = −0.1) indicating that this single reference Hartree–Fock wave function does not have sufficient flexibility to describe this molecule correctly. At UHF level, we found two different wave functions that described the electron structure of ZnO. The first open shell wave function has one electron in the 4*s* orbital of the Zn atom and the second one in a *p*-orbital forming the Zn—O bond as in **1**. In the other open shell configuration, the unpaired electron on the oxygen was in a *p*-orbital perpendicular to the Zn—O bond axis, **2**. These two wave functions are 35.3 and 44.2 kcal/mol below the energy of the closed shell wave function. Both wave functions have a large spin contamination; $\langle S^2 \rangle = 0.887$ and $\langle S_2 \rangle = 1.008$. Reoptimization of the Zn—O bond distances for these open shell wave functions gave bond distances of 1.717 and 1.797 Å, respectively. The energy of singlet **2** is 13.2 kcal/mol lower than that of **1**.

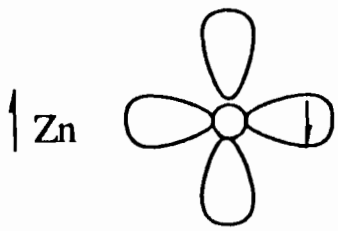

1

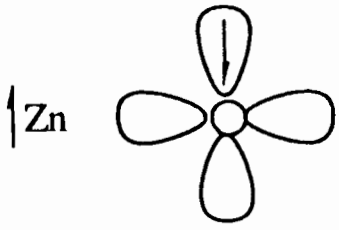

2

Multireference schemes such as the complete active space SCF (CASSCF) method are capable of overcoming the inadequacies of the Hartree–Fock model by providing a general treatment of the internal correlation problem. In the CASSCF representation, these low-lying biradicals will manifest themselves as different roots of the multiconfigurational secular problem with orbitals being optimized for the lowest root.

The UHF natural orbitals for each of the above wave functions corresponding to **1** and **2** were used to initiate the CASSCF calculation with the 3-21G basis set. The active space included the 4*s* orbital of the Zn atom and the three *p* orbitals on oxygen (four orbitals, six electrons). The wave function for biradical **1** (Zn—O = 1.717 Å) had the lowest root with an energy of −1843.369702 a.u. and CI coefficients of 0.9042 and −0.4259 for the $\pi_x^2\pi_y^2\sigma^2\sigma^*$ and $\pi_x^2\pi_y^2\sigma\sigma^{*2}$ configurations. A natural orbital population analysis gave 1.645 and 0.357 electrons for the σ^* and σ Zn—O orbitals, respectively, for **1**.

Since one of the main weaknesses of multiconfigurational schemes is the difficulty involved in treating the dynamic correlation, the two Zn—O configurations (**1** and **2**) were optimized with correlation at the UMP2 level with the DZP basis set. At this level, Zn—O bond distances of 1.772 and 1.841 Å are predicted for **1** and **2**, respectively, and configuration **2** was 14.9 kcal/mol more stable than **1** when spin projection was included (PM2/WH).

Table 1.
Total energies (a.u.) for reactants, complexes, and transition states, and the relative energies (ΔE, kcal/mol) for reaction paths 1 and 2 for the oxygen insertion from zinc oxide to ethylene

Stationary points	HF/3-21G	ΔE	CISD/3-21G// HF/3-21G	ΔE	UHF/3-21G// HF/3-21G	CASSCF(8,8)// HF/3-21G	ΔE
3	−1920.93716	0.00	−1921.41395	0.00	unstable	−1921.25904	0.0
TS-1	−1920.92323	8.74	−1921.39850	9.70	−1920.993841	−1921.24122	11.18
4	−1921.00972	−45.54	−1921.46392	−31.36	stable	−1921.29168	−20.49
TS-2	−1920.92150	9.82	−1921.38054	20.96	−1920.964081	−1921.21792	25.80
5	−1920.96994	−20.56	−1921.41572	−1.11	stable	−1921.24518	8.69
TS-3	−1920.89483	26.56	−1921.36069	33.42	−1920.94957		
Reactants	−1920.89944	23.66	−1921.36802[a]	28.82	unstable		
Products	−1920.94918	−7.55	−1921.39230[a]	13.58	stable		

[a] These energies of reactants and products were computed with a distance of 10 Å between fragments.

3.2. Oxygen atom transfer from ZnO to ethylene

There are at least two potential pathways for the epoxidation of ethylene by ZnO. In the first approach that we investigated, we found a reactant cluster involving a π-type complex of the zinc with the ethylene π-bond at the HF/3-21G level. Complex **3** was 23.7 kcal/mol below its isolated reactants (Table 1). The barrier height for the rearrangement of this minimum to metallocycle **4** was 8.7 kcal/mol. The cyclic ZnO–ethylene adduct was predicted to be 69.2 kcal/mol lower in energy than its isolated reactants. The activation energy for rearrangement of metallocycle **4** to zinc-coordinated ethylene oxide **5** via **TS-2** was calculated to be 55.4 kcal/mol. The overall change in energy for this 'oxygen tumbling' process affording zinc-coordinated ethylene oxide from reactant cluster **3** is exothermic by 7.5 kcal/mol.

Because of the biradical nature of the ZnO, monomeric cluster **3**, **TS-1**, and **TS-2** exhibited an RHF→UHF instability with roots of −0.07, −0.16 and −0.10, respectively. The metallocycle **4** and product complex **5** had stable wave functions. As demonstrated in Fig. 1, a CISD calculation on the HF/3-21G geometries (CISD/3-21G//HF/3-21G) did not markedly affect the overall potential energy surface. However, at the CASSCF level, the potential energy surface was markedly different, as one might anticipate. The active space for these intermediates included the bonding and antibonding combination of the C—C double bond, the Zn—O sigma bond, and the Zn—O π_x and π_y orbitals (eight electrons, eight orbitals). The structures that had RHF→UHF unstable wave functions exhibited the greatest energy stabilization with the CASSCF wave function. At the CASSCF/3-21G level the barrier heights for **TS-1** and **TS-2** are 11.2 and 25.8 kcal/mol, respectively (Fig. 1).

We also briefly examined the epoxidation pathway involving direct displacement of an oxygen atom from ZnO by nucleophilic attack by the ethylene π-bond (Fig. 2). However, at the CISD/3-21G level, **TS-3** is 12.5 kcal/mol higher in energy than **TS-2**. Intrinsic reaction coordinate (IRC) following [11c] in both directions from the transition state did suggest that **TS-3** was connected to reactants ethylene and ZnO and product ethylene oxide (Fig. 2).

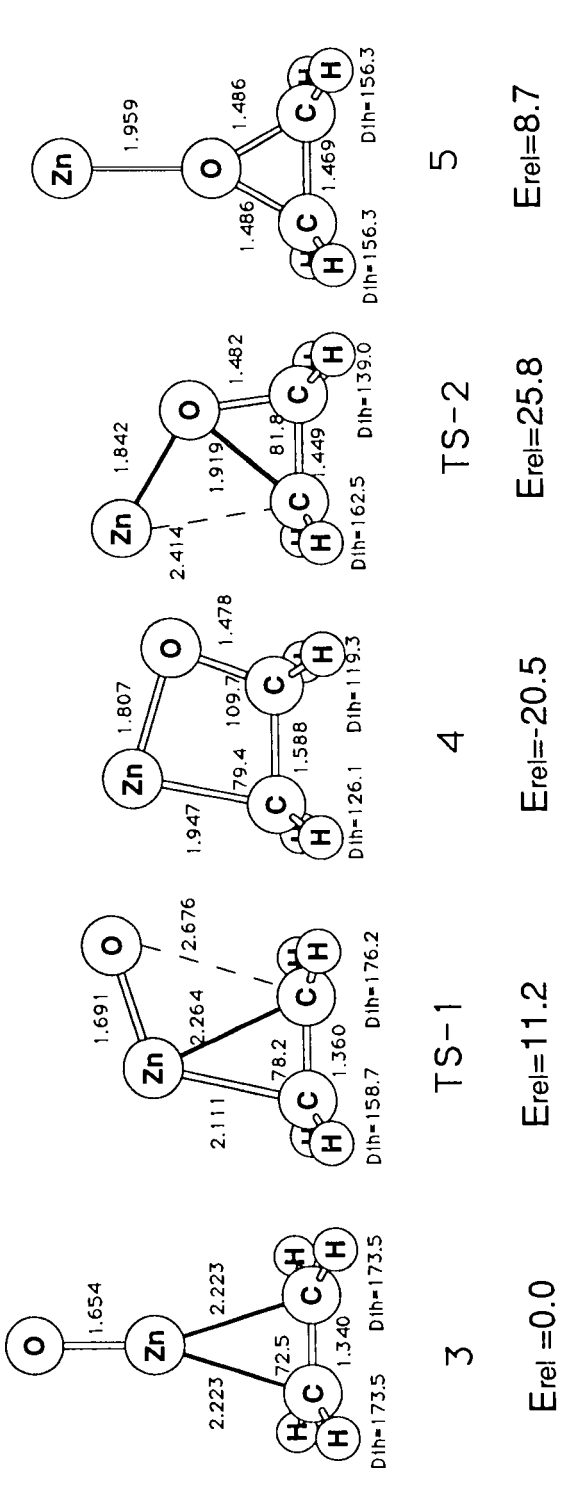

Figure 1. Reaction path 1 for the oxygen insertion from zinc oxide to ethylene calculated at the HF/3-21G level. Bond lengths are given in Å and angles in degrees. The dihedral angles (Dih) are defined around the carbon atoms as H—C—C—H. Relative energies (in kcal/mol) were computed at the CAS/3-21G level using the HF/3-21G geometry.

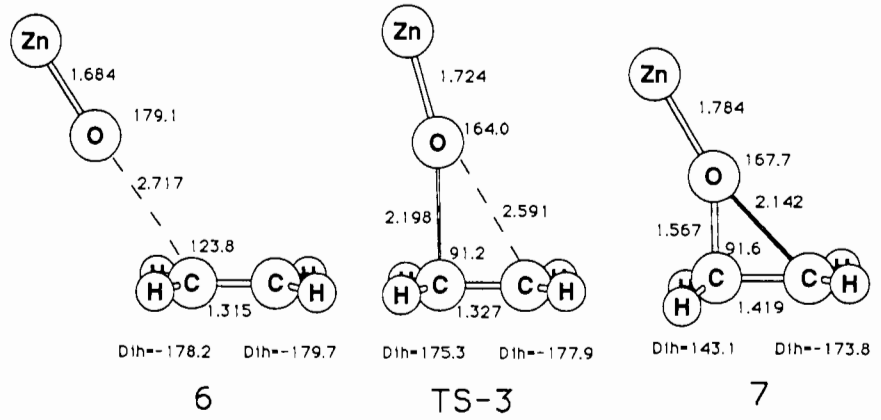

Figure 2. Transtition state and two intermediate points along reaction path 2 for oxygen insertion from zinc oxide to ethylene calculated at the HF/3-21G level. Energies recalculated at both CISD/3-21G and CASSCF/3-21G levels. Bond lengths are given in Å, angles in degrees. Structure **6** is 2.78 kcal/mol below **TS-3** with a displacement of 2.0 a.u. along the IRC, and structure **7** is 12.2 kcal/mol below **TS-3** with a displacement of 1.0 a.u.

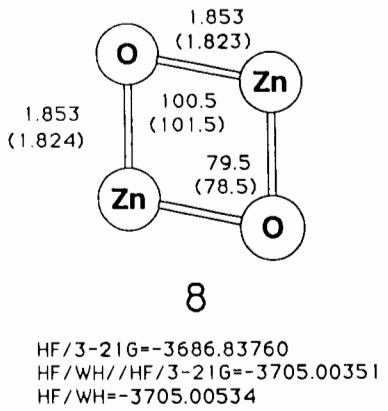

Figure 3. Structure of the zinc oxide dimer calculated at both HF/3-21G (values in parentheses) and HF/WH levels. Bond lengths are given in Å, angles in degrees, and total energies in a.u.

3.3. Reactions of zinc oxide dimer

The above problems with the open shell or biradical nature of ZnO suggested that its dimeric form may be less problematic. This modification may also present a structure that could serve as a model for the zinc oxide surface. The geometry of dimer **8** was initially optimized at the HF/3-21G level and then fully optimized at the HF/WH level. The two basis sets showed quite good agreement (Fig. 3) and the wave functions for the dimeric structure was RHF→UHF stable in both cases.

Ethylene complexation with dimer **8** formed a relatively stable π-complex **9** (Fig. 4) with a binding energy of 24.9 kcal/mol at the MP2/WH level (Table 2). Insertion of ethylene into the zinc dimer forming cyclic adduct **10** had a surprisingly low activation

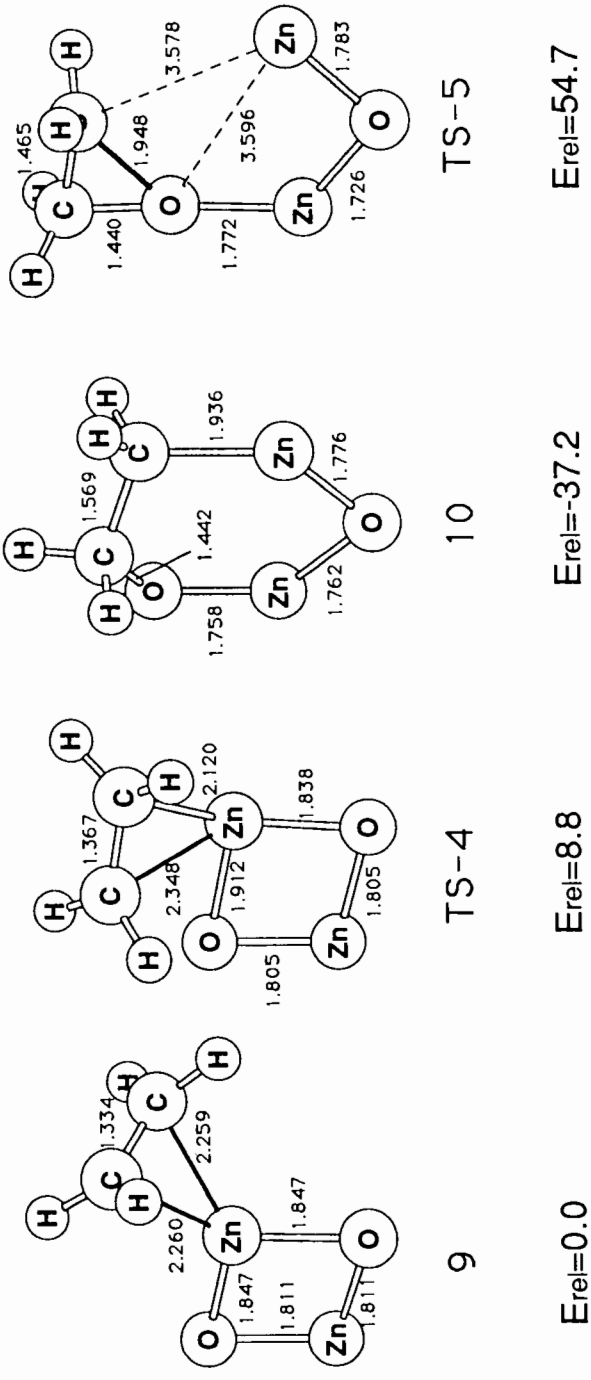

Figure 4. Ethylene insertion into zinc oxide dimer. Geometries have been optimized at the HF/3-21G level. Bond lengths are given in Å and angles in degrees. Relative energies (in kcal/mol) were computed at the MP2/WH level using the HF/3-21G geometry.

Table 2.
Total energies (a.u.) for reactants, complexes, and transition states, and potential barriers (ΔE, kcal/mol) for the reactions between zinc oxide dimer and ethylene, ammonia, and water

Stationary points	HF/3-21G	ΔE	HF/WH// HF/3-21G	ΔE	MP2/WH// HF/3-21G	ΔE
$(ZnO)_2 + C_2H_4$						
9	−3764.81647	0.00	−3783.07584	0.00	−3784.17460	0.00
TS-4	−3764.81013	3.98	−3783.05747	11.53	−3784.16053	8.82
10	−3764.88623	−43.78	−3783.14353	−42.48	−3784.23391	−37.21
TS-5	−3764.71936	60.93	−3782.99320	51.85	−3784.08750	54.66
Reactants	−3764.77243	27.63	−3783.05238	14.72	−3784.13489	24.92
$(ZnO)_2 + NH_3$						
11	−3742.79638	0.00	−3761.24989	0.00	−3762.25792	0.00
TS-6	−3742.78986	4.09	−3761.22869	13.30	−3762.24268	9.56
Reactants	−3743.04365	53.16	−3761.19954	31.60	−3762.19665	38.45
$(ZnO)_2 + 2\ NH_3$						
13	−3798.71950	0.00	−3817.46524	0.00	−3818.65345	0.00
TS-7	−3798.71151	5.02	−3817.44352	13.63	−3818.64279	6.69
Reactants	−3798.58200	86.28	−3817.39743	43.13	−3818.56018	58.53
$(ZnO)_2+H_2O+NH_3$						
14	−3818.45041	0.00	−3837.30894	0.00	−3838.51335	0.00
TS-8	−3818.45029	0.08	−3837.30571	2.03	−3838.51098	1.49
Reactants	−3818.29576	97.00	−3837.23330	47.47	−3838.41468	61.92

barrier of 8.8 kcal/mol (Fig. 4). The geometry of the transition state (**TS-4**) for this insertion process did not differ significantly from reactant cluster **9** with the exception of migration of the ethylene fragment across the Zn—O bond. Product **10** was 37.2 kcal/mol lower in energy than reactant complex **9**. Single point calculations at the MP2/WH level did not have a marked effect on the relative energies. These data suggest that insertion reactions of alkenes into the zinc oxide surface should prove to the quite facile. As noted above for the potential energy surface involving monomeric ZnO, we also found a pathway for rearrangement of complex **10** that involved the formation of ethylene oxide. This transition state (**TS-5**) was 54.7 kcal/mol above the ground state and involved significant molecular reorganization. The wave function for **TS-5** was RHF→UHF unstable with a root equal to −0.16. Both **TS-4** and the cyclic adduct **10** were RHF→UHF stable.

Zinc oxide dimer **8** also formed a stable complex with ammonia **11** (Fig. 5). The stabilization energy at the HF/WH level on the HF/3-21G geometry (HF/WH//HF3-21G) was calculated to be 38.5 kcal/mol. The activation barrier for insertion of the NH_3 molecule into the dimer forming Zn—NH_2 and O—H bonds is predicted to be 9.6 kcal/mol when the barrier height is measured from reactant cluster **11**. The Zn—O bond in **TS-6** has been elongated by 0.15 Å and the N—H bond is elongated by about 20%. The structure of the final product **12** was not fully optimized because the molecule is very 'floppy' and convergence in the geometry optimization proved to be difficult.

Aminolysis of dimer **8** with two ammonia molecules was also studied in an effort to model the interaction of a diamine with a zinc oxide surface. The binding energy of

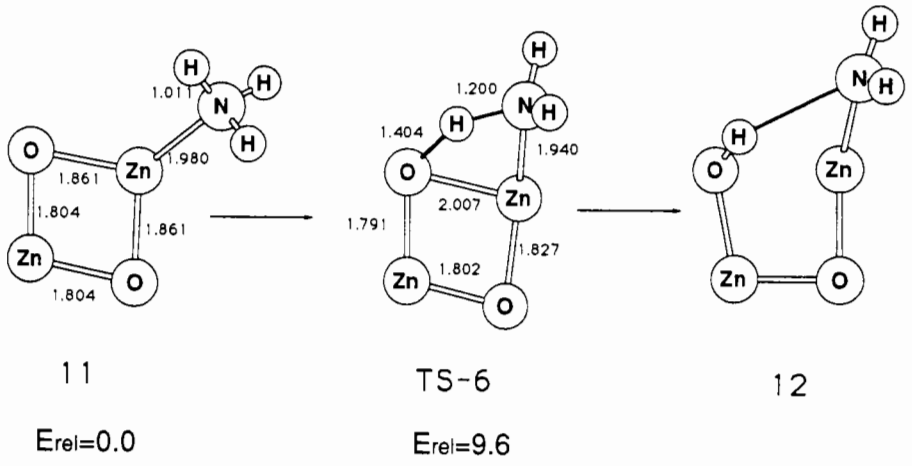

Figure 5. Aminolysis of zinc oxide dimer. Geometries have been optimized at the HF/3-21G level. Bond lengths are given in Å and angles in degrees. Relative energies (in kcal/mol) were computed at the MP2/WH level using the HF/3-21G geometry.

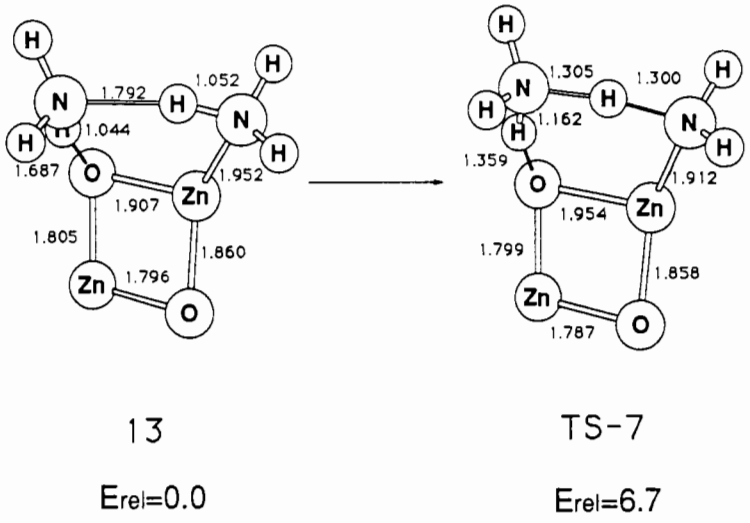

Figure 6. Aminolysis of zinc oxide dimer with two molecules of ammonia. Geometries have been optimized at the HF/3-21G level. Bond lengths are given in Å and angles in degrees. Relative energies (in kcal/mol) were computed at the MP2/WH level using the HF/3-21G geometry.

the hydrogen-bonded complex **13** was 58.5 kcal/mol (Fig. 6). One NH_3 was bonded to the zinc atom and the other was hydrogen-bonded to the oxygen with a fairly short O—H bond length of 1.687 Å. The activation barrier for breaking the Zn—O bond and forming the ammonia complex (**TS-7**) was predicted to be 6.7 kcal/mol (3 kcal/mol lower than with one ammonia). We also examined the binding characteristics of a

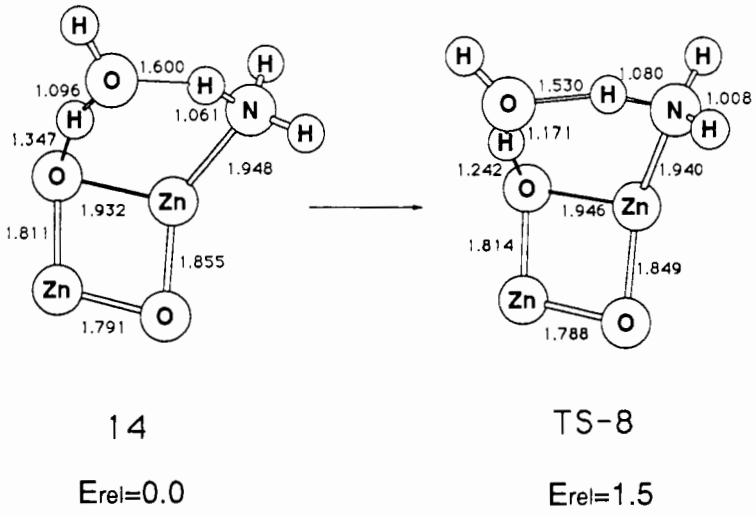

Figure 7. Aminolysis of zinc oxide dimer with water and ammonia. Geometries have been optimized at the HF/3-21G level. Bond lengths are given in Å and angles in degrees. Relative energies (in kcal/mol) were computed at the MP2/WH level using the HF/3-21G geometry.

complex between dimer **8** and a molecule of ammonia and water **14** (Fig. 7). The transition structure (**TS-8**) for Zn—O bond rupture with one NH_3 and one H_2O molecule closely resembled **TS-7** and the activation barrier was surprisingly low (1.5 kcal/mol). Presumably, the difference in barrier heights for **TS-7** and **TS-8** is a reflection of the greater acidity of water relative to ammonia.

4. CONCLUSION

In summary, the wave functions for the dimer of zinc oxide, **8**, its reactant clusters, and transition states, with the exception of **TS-5**, were all RHF→UHF stable. Consequently, model surface interactions with organic molecules are feasible at the *ab initio* level when the dimer of zinc oxide is used to model the metal oxide surface. These data suggest that insertion reactions of carbon-carbon double bonds into the Zn—O bond should be quite feasible. The relatively low activation energies for aminolysis and hydrolysis also suggest that amines, water, or alcohol functional groups should be quite capable of forming covalent bonds with the ZnO surface.

Acknowledgement

This work was supported in part by a grant from the National Science Foundation (CHE-90-20398) and the National Institutes of Health (CA 47348-02). We are very grateful to the Ford Motor Company, the Pittsburgh Supercomputing Center, and to Cray Research for generous amounts of computing time. One of us (JLA) acknowledges the CIRIT of the Generalitat Catalunya (Catalonia, Spain) for financial support.

REFERENCES

1. S. R. Cain, *J. Adhesion Sci. Technol.* **4**, 333 (1990).
2. S. R. Cain and L. J. Matienzo, *J. Adhesion Sci. Technol.* **2**, 395 (1988).
3. R. Hoffmann, *Solids and Surfaces: A Chemist's View of Bonding in Extended Structures.* VCH, New York (1988).
4. J. W. Holubka, R. A. Dickie and J. C. Cassatta, *J. Adhesion Sci. Technol.* **6**, 243 (1992).
5. J. W. Holubka and J. C. Ball, *J. Adhesion Sci. Technol.* **4**, 443 (1990).
6. (a) B. LeFez and M. Lenglet, *Chem. Phys. Lett.* **179**, 223 (1991).
   (b) K. Wada, K. Yoshida, Y. Watanabe and T. Suzuki, *J. Chem. Soc. Chem. Commun.*, 727 (1991).
   (c) S. V. Didziulis, S. L. Cohen, K. D. Butcher and E. I. Solomon, *Inorg. Chem.* **27**, 2238 (1988).
   (d) J. A. Rodriguez and C. T. Campbell, *J. Phys. Chem.* **91**, 6648 (1987).
   (e) R. Baetzold, *J. Phys. Chem.* **89**, 4150 (1985).
   (f) H. Lüth, G. W. Rubloff and W. D. Grobman, *Surface Sci.* **74**, 365 (1978).
   (g) G. W. Rubloff, H. Lüth and W. D. Grobman, *Chem. Phys. Lett.* **39**, 493 (1976).
7. M. H. Sukkar, K. H. Johnson and H. L. Tuller, *Mater. Sci. Eng.* **B6**, 49 (1990).
8. A. B. Anderson and D. Q. Dowd, *J. Phys. Chem.* **91**, 869 (1987).
9. V. M. Allen, W. E. Jones and P. D. Pacey, *Surface Sci.* **220**, 193 (1989).
10. S. F. Jen and A. B. Anderson, *Surface Sci.* **223**, 119 (1989).
11. (a) M. J. Frisch, G. W. Trucks, M. Head-Gordon, P. M. W. Gill, M. W. Wong, J. B. Foresman, B. G. Johnson, H. B. Schlegel, M. A. Robb, E. S. Replogle, R. Gomperts, J. L. Andres, K. Raghavachari, J. S. Binkley, C. Gonzalez, R. L. Martin, D. J. Fox, D. J. Defrees, J. Baker, J. J. P. Stewart and J. A. Pople, *GAUSSIAN 92.* Gaussian, Inc., Pittsburgh, PA (1992).
    (b) H. B. Schlegel, *J. Computational Chem.* **3**, 214 (1982).
    (c) C. Gonzalez and H. B. Schlegel, *J. Chem. Phys.* **90**, 2154 (1989).
12. K. D. Dobbs and W. J. Hehre, *J. Computational Chem.* **8**, 861 (1987).
13. (a) A. J. H. Wachters, *J. Chem. Phys.* **52**, 1033 (1970).
    (b) J. P. Hay, *J. Chem. Phys.* **66**, 4377 (1977).
    (c) R. F. Stewart, *J. Chem. Phys.* **52**, 431 (1970).
    (d) S. Huzinaga, *J. Chem. Phys.* **42**, 1293 (1965).
    (e) T. H. Dunning, *J. Chem. Phys.* **53**, 2823 (1970).